Vivaldi Tapered Slot Antenna for Microwave Imaging in Medical Applications

Randy Ivanal Hakim, Daffa Mahendra, and Endarko*

Laboratorium Fisika Medis dan Biofisika, Departemen Fisika, Institut Teknologi Sepuluh Nopember

Kampus ITS Sukolilo – Surabaya, Jawa Timur, 60111, Indonesia

**Corresponding author. Email: endarko@physics.its.ac.id*

Abstract— Microwave imaging has become an active research area in recent years, owing primarily to advancements in detecting the early stages of cancer. The study aimed to create a high-gain compact Vivaldi Tapered Slot antenna (VTSA) for microwave imaging in medical applications and also aims to address several challenges in the development of microwave imaging (MWI) technology for medical applications. These challenges include the ability to detect and identify abnormalities in human tissue and considering safe Specific Absorption Rate (SAR) limits for patients, the approach of balancing of penetration and resolution can be done on the design. The antenna operates at frequencies ranging from 1.7 to 3.1 GHz and is built on a low-cost Flame Retardant-4 (FR-4) substrate with a thickness of 1.6 mm. A compact exponential VTSA is initially presented while designing the proposed antenna for broad impedance bandwidth performances. The simulation used a back-to-back linear array of antennas with or without a phantom, specifically a without phantom (only antennas), a water phantom (cube shape), and an anomaly inside the water phantom. The results revealed a significant shift in the signal graph between the three results, indicating a difference in values between the three simulations. A transient domain solver calculation was used in the simulation. The designed antenna improved a gain of 6.09 dBi and a SAR of 0.326 W/kg by maximizing the edges of the exponential in the tapered section and the feedline slot area. The antenna exhibits differences in scattering parameters on each simulation of anomalies across the required frequency range. The result finds suitability of the experiment and simulation in assessing the microwave imaging capabilities. With the data presented, simulated antennas can be used for microwave imaging. The next study should aim on making a suitable imaging system with dimensions that supported in the antenna range and specifications.

Keywords— FR-4; microwave imaging; specific asorption rate; vivaldi antenna

I. INTRODUCTION

Conventional imaging techniques, such as X-ray, ultrasound, and magnetic resonance imaging (MRI), have long been used in medical diagnostics. While these methods have been successful in many cases, they also have limitations, particularly in terms of their ability to accurately detect and characterize certain types of abnormalities, such as small tumors or lesions. This has led to the exploration and development of microwave imaging as an alternative approach. Microwave imaging can be a safe and effective method for diagnosing human tissue abnormalities. It has several advantages over traditional radiology methods, including non-ionizing, non-invasive, and relatively inexpensive. These benefits make it a promising alternative for medical imaging, particularly for patients unable to undergo traditional radiological methods due to health [1].

Microwave imaging is a technique that uses microwave radiation to create images of the internal structure of biological tissues. It emits low-power microwave radiation toward the tissue of interest and measures the reflected signal. By analyzing the changes in the signal, an image of the tissue's internal structure can be created [2].

One of the key advantages of microwave imaging is its non-ionizing and non-invasive nature, which makes it safer for patients compared to traditional radiology methods that use ionizing radiation. Additionally, it is relatively inexpensive compared to other medical imaging techniques, making it more accessible for patients [3].

Microwave imaging has been used for various medical applications, including breast cancer detection and monitoring, brain imaging, and skin cancer detection. It has shown promising results in these areas, with high accuracy rates and low false positive rates [4].

Microwave imaging, like any new technology, has limitations and challenges. One of the main challenges is that microwave signals have a lower resolution and a limited penetration depth when compared to ionizing radiation, which may limit their ability to detect small abnormalities or those located deep within the body. Furthermore, factors such as tissue heterogeneity, tissue movement, and the presence of other objects in the imaging area can all affect the accuracy of imaging results [5].

Despite these challenges, research and development in microwave imaging continue to show encouraging results, and the technology is progressively being incorporated into clinical practice. With continued development and improvement, microwave imaging has the potential to play a significant role in the diagnosis and follow-up of many illnesses, particularly those connected to breast cancer, brain tumors, and skin conditions [5], [6].

In microwave imaging applications, various types of antennas are utilized, including patch antennas, horn antennas, microstrip antennas, dipole antennas, slot antennas, and many more. These antennas offer different characteristics and

Received 15 April 2023, Revised 27 September 2023, Accepted 17 October 2023.

DOI: https://doi.org/10.15294/jte.v15i2.43955

performance capabilities for imaging purposes. However, Vivaldi antennas have gained significant attention in recent years due to their unique advantages. Vivaldi antennas, also known as tapered slot antennas, are particularly well-suited for microwave imaging applications. They offer wide bandwidth, high gain, and directional radiation patterns, making them ideal for capturing and detecting fine details in imaging scenarios. The exponential taper design of Vivaldi antennas allows for enhanced impedance matching and improved radiation efficiency. Moreover, their compact size and ease of integration make them suitable for portable and wearable imaging devices. Vivaldi antennas offer excellent performance in terms of resolution, sensitivity, and imaging depth, making them a popular choice in the field of microwave imaging [7].

The Vivaldi Tapered Slot Antennas (VTSA) has an exponential slot that runs from the feed point to the antenna's edge. Because of its wide bandwidth and high gain, this design is ideal for high-resolution imaging applications. This antenna, however, is susceptible to cross-polarization and sidelobe radiation [8], [9].

Due to its high gain and bandwidth, the VTSA is a popular choice for microwave imaging (MWI) systems. The linear stepped slot design of the antenna allows for smooth transitions between different parts of the antenna, minimizing reflection loss and improving overall performance. Various techniques, namely using different substrates, modifying the shape and size of the antenna elements, and adding parasitic elements, have been proposed to improve the impedance match and radiation pattern of the VTSA for MWI systems [9].

One of the key considerations in microwave imaging is the selection of an appropriate frequency range that offers optimal performance for the intended application. In this regard, the frequency range of 1.7 - 3 GHz has garnered significant attention for microwave imaging applications. The 1.7 - 3 GHz frequency range holds great potential for microwave imaging due to its unique characteristics and capabilities. It offers a balance between resolution and penetration depth, making it suitable for a range of imaging scenarios. This frequency range allows for the imaging of both superficial and deeper structures within the target medium. In the field of medical imaging, the 1.7 - 3 GHz range has shown promise for detecting early stages of diseases, including cancer. The ability of microwave signals in this frequency range to penetrate biological tissues, combined with their sensitivity to dielectric properties, enables the detection of anomalies and abnormalities with visible contrast. This makes it an attractive option for early-stage imaging, where the focus is on identifying subtle variations in tissue properties [7].

The SAR limit value of 1.6 W/kg is an important safety standard for MWI systems because it ensures that the amount of electromagnetic energy absorbed by the body is safe. The SAR value is determined by the frequency of the microwave signal as well as specific body tissue properties such as dielectric constant and conductivity [10]. Because of its high gain and bandwidth, VTSA is a promising choice for MWI systems. Vivaldi antennas are still being designed and optimized for MWI applications, making them a reliable and effective tool for medical imaging. As previously stated, a high-gain VTSA with a SAR value within safe limits for medical applications was investigated in this study. S11 and S21 values were also investigated to analyze the performance designed VTSA for recognizing objects using phantom.

This research aims to address several challenges in the development of MWI technology for medical applications. These challenges include the ability to detect and identify abnormalities in human tissue and considering safe Specific Absorption Rate (SAR) limits for patients. In this context, the research problem formulation involves questions about how to improve the performance of VTSA in MWI systems while taking these limitations into account.

This study makes a significant contribution by presenting the design and modeling of VTSA with high performance in microwave imaging systems. The main contribution is in enhancing resolution, sensitivity, and imaging depth in medical imaging applications. The developed VTSA design in this research provides superior performance in terms of impedance matching and radiation pattern, minimizing signal loss. The research also considers safe SAR limits for medical applications, ensuring that electromagnetic energy absorbed by the body remains within safe boundaries.

The proposed VTSA design in this research offers several novelties. Firstly, it achieves high performance in terms of resolution and sensitivity in MWI applications. Secondly, this VTSA is designed while considering safe SAR limits, making it more suitable for medical applications. Thirdly, the design approach maximizes radiation efficiency, reduces signal loss, and improves image quality. The novelty of this design makes VTSA a reliable and effective tool in medical imaging, with the potential to better identify abnormalities and anomalies in the human body compared to similar products previously available.

II. METHOD

A. Design

As shown in Figure 1, the VTSA in this study made using FR-4 Flame Retardant-4 (FR-4) substrate with a thickness of 1.6 mm and an impedance of 50 Ω. The patch antenna's "a" curve (the exponential part with the length curve) is calculated using the following equation [11]:

$$y = C_1 . e^{(ax)} + \frac{wh}{2} - C_1 \quad (1)$$

$$C_1 = \frac{\frac{w3}{2} - \frac{wh}{2}}{e^{(al)} - e^{(a0)}} \quad (2)$$

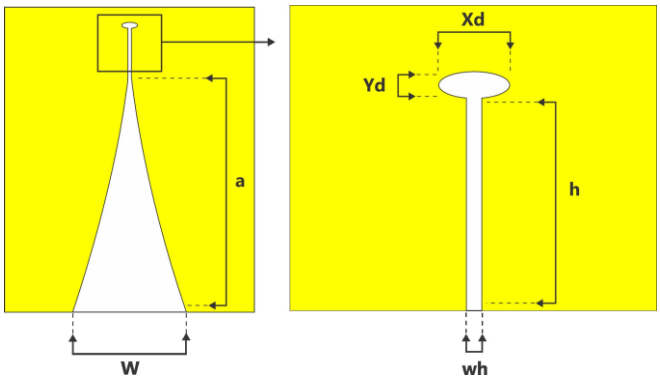

Figure 1. VTSA template design in this study

The equation (1) represents a curve in a two-dimensional plane acting as a medium. Here, the x-axis represents the input variable, while the y-axis represents the corresponding output variable. The curve is shaped by the exponential function $C_1e^{(ax)}$, which determines its growth or decay pattern with the rate of change determined by the constant a. The additional terms, wh/2 and $-C_1$, contribute to the curve's horizontal and vertical shifts, respectively, affecting its position along the x-axis and y-axis. By manipulating the values of C_1, a, and wh/2, we can study different aspects of the curve within this medium, analyzing the relationship between the input and output variables and exploring the effects of changes in the input on the resulting output.

The patch antenna's exponential curvature is used to achieve a more gradual change in width, which helps to reduce impedance mismatch between the antenna and the transmission line. As a result, the bandwidth is increased, the radiation characteristics are improved, and the gain is increased.

In this method, the antenna's design parameters are adjusted iteratively until the desired performance specifications, such as bandwidth, gain, and directivity, The bandwidth should be more than 50% on working frequency with gain and directivity of more than 5 dBi. The design parameters are then adjusted based on the simulation results, and the process is repeated until the desired performance specifications are met. This iterative process allows for a more precise optimization of the antenna's design parameters, resulting in a more efficient and effective design, the parameters summarized in Table I.

TABLE I. PARAMETERS DESIGN FOR VTSA IN THE STUDY

Parameter	Description
l	Length of substrate
w	Width of substrate
w3	Half width of substrate
Xd	Ellipse length
wh	Slot Width
a	Exponential constant
h	Slot Length
Yd	Ellipse width

B. Measurement of S11 and S21

Figure 2 depicts the design setup used in this study for VTSA performance testing to obtain S11 and S21 values. In Figure 2 (a), a single antenna simulation with a time domain solver with -20dB accuracy and 50-ohm impedance is used to calculate the S11 parameter, with a frequency range of 1.5–4 GHz for simulating the S11 parameters on a single receiving and transmitting antenna with magnitude in dB of each frequency range in Ghz. All three S21 calculation simulations used three variations: (b) without phantom, (c) water phantom with a dimension of 50×50×50 mm^3, and (d) water phantom with anomalies with a spherical diameter of 20 mm. We used the same setting solver with a frequency range of 1.7–3 Ghz for simulating the S21 parameters on each receiving and transmitting antenna with magnitude in dB of each frequency range in Ghz.

Figure 3 illustrates the experimental setup employed in this study to evaluate the performance of the VTSA and obtain S11 and S21 values. The experiment was carefully designed to ensure accurate measurements and reliable data acquisition. The setup involved placing two antennas at a fixed distance of 8 cm apart, creating a back-to-back configuration. This arrangement allowed for the evaluation of the antenna's characteristics, including its reflection and transmission properties. To measure the S-parameters, a Vector Network Analyzer (VNA) with a frequency range of 1.5-3 GHz was utilized. The VNA provided precise control over the frequency sweep and offered high-resolution measurements. By connecting the VNA to the antennas, the incident and transmitted signals could be analyzed, allowing for the determination of the scattering parameters S11 and S21. These parameters provided insights into the antenna's impedance matching, radiation efficiency, and signal transmission performance. Throughout the experiment, great care was taken to minimize external interference, maintain stable measurement conditions, and ensure accurate positioning of the antennas. The obtained S-parameter data served as valuable information for evaluating the VTSA's performance and assessing its suitability for microwave imaging applications.

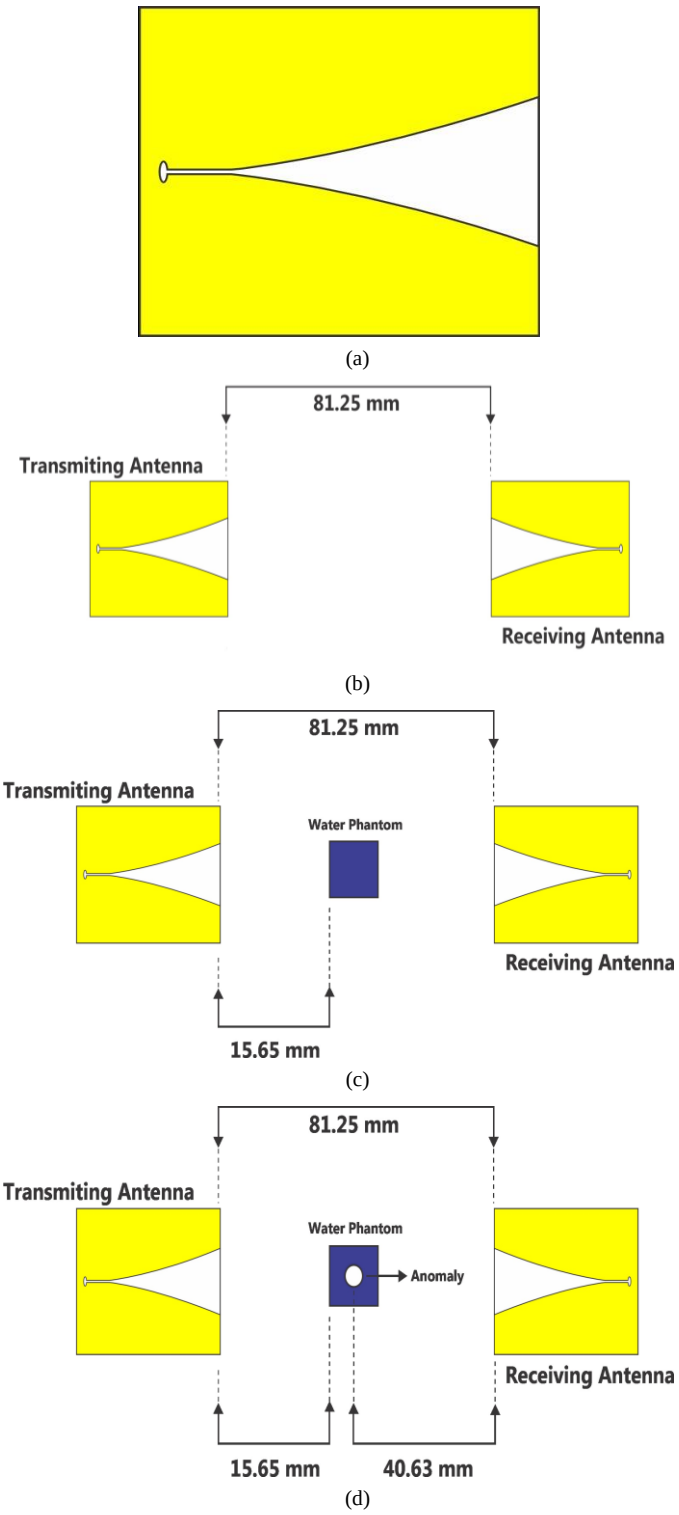

Figure 2. Setup design for measurement S11 and S21 values: (a) S11 parameter with single antenna simulation, (b) S21 parameter simulation without fantom, (c) S21 parameter simulation with water fantom, and (d) S21 parameter simulation with water anomalies fantom

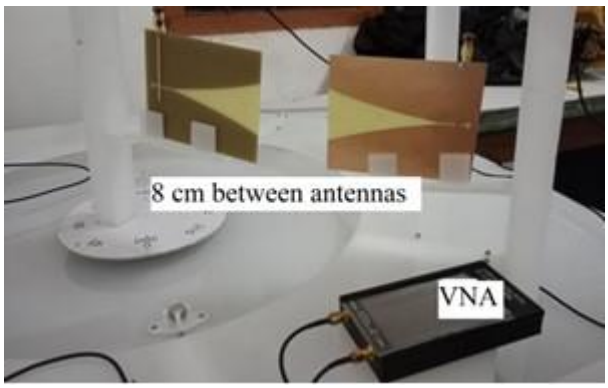

Figure 3. Setup for measurements S11 and S21 values

C. Specific Absorption Rate (SAR)

The SAR method is commonly used in bio electromagnetics to study the potential effects of electromagnetic radiation on human health. The SAR is expressed in watts per kilogram (W/kg). In this study, the SAR was mathematically calculated using the equation as follows [12]:

$$SAR = \frac{\sigma . E^2}{\rho} \quad (3)$$

Where σ indicates the value of the conductivity of the tissue (S/m), E represents the value of the internal electromagnetic energy (V/m), and ρ is the density of the tissue mass (kg/m^3) [10], [12].

In the process of calculating SAR using CST simulation, a comprehensive methodology is employed. The solver in CST is employed to solve Maxwell's equations and calculate the electromagnetic fields within the human tissues. These fields drive the interaction between electromagnetic waves and the tissues, leading to energy absorption and SAR generation. By utilizing the simulation results, SAR values are extracted and analyzed. It is important to ensure convergence of the simulation and validate against known benchmarks or experimental data to ensure accuracy.

Iterative adjustments to simulation parameters, mesh refinement, and model calibration may be necessary to enhance the precision of SAR calculations. The CST software offers tools for visualizing and analyzing SAR distributions within the tissues, aiding in the assessment of potential hotspots and areas of concern.

III. Results and Discussion

Figure 4 depicts the study's optimum design and the Figure 5 is the fabricated antenna, which uses all of the parameters listed in Table II to achieve a wide output bandwidth, high gain, and effective radiation direction when imaging.

The length and width of the substrate used for the antenna design are critical factors that determine the antenna's performance at a specific frequency range. The half-width of the substrate is proportional to the taper of the antenna and can be adjusted to control the antenna's impedance. It is advisable to consider alternative substrate materials that are better suited for higher frequencies and offer low loss but for this study we use FR-4 as it is commonly used substrate material for its low cost, high mechanical strength, and good electrical properties. It has a relative permittivity of around 4.4, which is relatively low compared to some other materials, making it suitable for applications where low dielectric loss is important. Low dielectric permittivity substrates are preferable as they reduce the levels of surface waves responsible for the degradation of antenna performance [5]. The dielectric constant also affects the dimensions of the antenna, as the wavelength of the signal is shortened when it travels through a material with a higher dielectric constant. This can lead to a smaller antenna size for a given operating frequency than a lower dielectric constant material [13].

The ellipse length and width are important design parameters that affect the antenna's radiation pattern. The antenna can be made to radiate in a specific direction or with a specific polarization by carefully selecting these values for this research with a width of 2 mm and length of 6 mm; other research with additional circular or ellipse slotting it shows better impedance, respectively on the width and length of the slot [11].

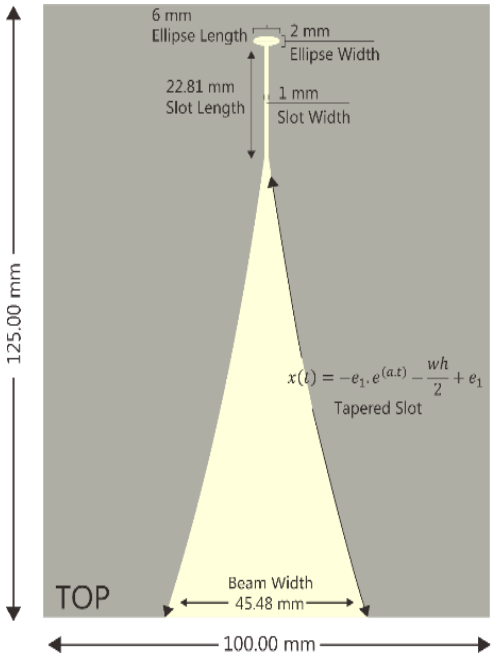

Figure 4. Resulted design of VTSA in this study

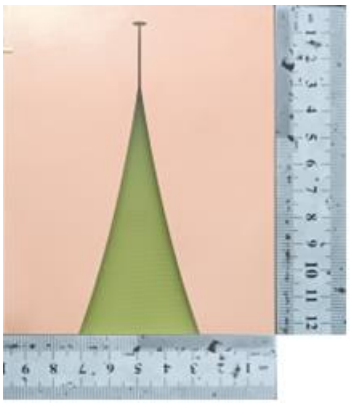

Figure 5. VTSA fabrication in this study

TABLE II. Optimum Values of Parameters Design in the Study

Parameter	Value (mm)
l	125
w	100
w3	50
Xd	6
wh	1
a	0.009
h	22.8
Yd	2

The slot width and length are optimized based on the desired frequency range, with wider slots resulting in a lower resonant frequency and narrower slots resulting in a higher resonant frequency. These values affect the antenna's impedance and can be used to tune it to a specific frequency range of 1.7 – 3 Ghz. The exponential constant is a parameter used to determine the antenna's curvature. Additionally, the exponential constant is selected based on the desired curvature of the antenna, with a higher value resulting in a more curved antenna and a lower value resulting in a less curved antenna. This value can be changed to control the antenna's shape and optimize its performance with a broader beam width of 45.48 mm, giving it a better direction on the radiation [14].

With the assessment of antenna performance, a comparative analysis was conducted between a simulated radiation pattern and a measured one obtained within a controlled chamber. The figures below showcase the radiation patterns of the antenna in question. Figure 6 illustrates the simulated radiation pattern, generated through software simulations and also displays the radiation pattern obtained from actual measurements. Remarkably, both patterns exhibit consistent back lobes and side lobes, indicating that the antenna's interactions with its surroundings remain stable across simulation and measurement. Notably, a slight disparity is observed in the main lobe's characteristics between the two patterns. This discrepancy can be attributed to factors such as inherent variations in the real-world environment, manufacturing tolerances, and potential inaccuracies in the simulation model. However, the alignment of the back lobes and side lobes underscores the reliability of both approaches in predicting unwanted radiations and interference. This comparative study underscores the significance of validating simulation results with empirical measurements and highlights the complex interplay between simulation accuracy and real-world conditions in antenna analysis similar to the results in the previous study review on [5].

The S11 graph in Figure 7 depicts the antenna's reflection coefficient on a return loss scale of -10 dB. The frequency at point 1 in the graph is 1.687 GHz with a reflection coefficient of -10 dB, while the frequency at point 2 is 3.1 GHz with a reflection coefficient of -10 dB. These are reference points for measuring several parameters, including the antenna's bandwidth and resonance frequency [15].

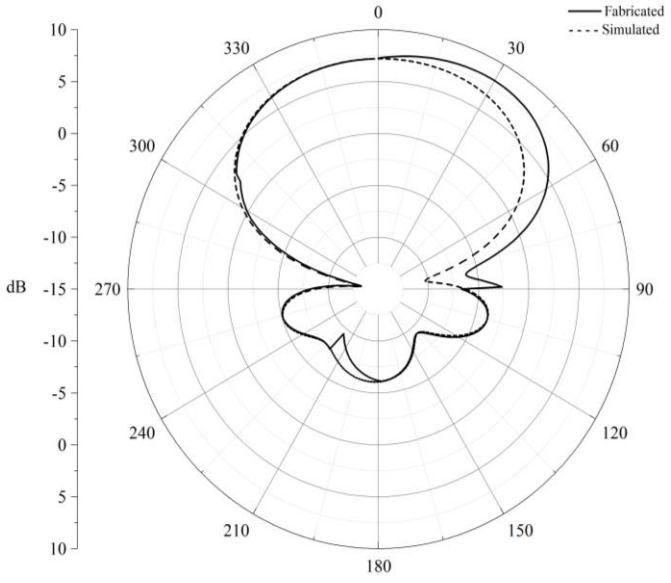

Figure 6. Simulated and fabricated VTSA radiation pattern

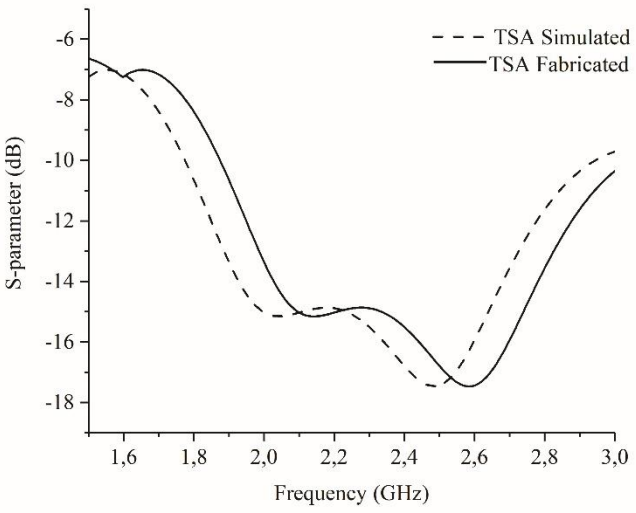

Figure 7. S-parameter (S11) characterization of simulated and real fabricated VTSA

With a return loss of -10dB, the reflected power is 10% of the incident power, while the remaining 90% is transmitted through the system. In other words, the power transfer efficiency from the source to the load is 90%. In microwave systems, a return loss of -10dB is typically desired because it indicates good impedance matching between the source and the load. When the return loss exceeds -10dB, it indicates more reflected power, indicating poor impedance matching and potential signal loss or system damage [11].

Table III is the result of simulation based measurement using CST so the data shows a gain value of 6.09 dB indicates that the antenna can amplify or focus signals in a front direction, whereas a directivity value of 6.95 dBi indicates that the antenna is capable of focusing energy in a front direction [9]. Gain and directivity is lower than previous study in the review stated that most of the Vivaldi antennas design have a gain of more than 7 dB up to 11 dB these values in the previous study, this study offers a smaller dimension and trying to find balance between limited field of view and precision spatial resolution in imaging [5]. The bandwidth value of 56.27% indicates the frequency range over which the antenna operates efficiently, this study choice in the band uses differ from previous which commonly have atleast 100% bandwidth, the study offers a smaller bandwidth which on the range of S-band (1-4 Ghz) but only covers the bandwidth with sufficient penetration on the targeted objects ranges . The target frequency of 2.29 GHz is the frequency at which the antenna is designed to operate far lower than the previous design [16], [17]. Furthermore, the negative return loss value of -17.09 dB indicates how much power has reflected the source due to impedance mismatch, with lower values indicating better performance [9].

TABLE III. OPTIMUM RESULTS OF PARAMETERS IN THE STUDY

Parameter	Value
VSWR	1.33
Gain	6.09 dB
Bandwidth	56.27%
Directivity	6.95 dBi
Frequency Target	2.39 GHz
Return Loss	-17.09 dB

When comparing two graphs of single S-parameters, it is essential to assess the impact of the differences observed. Both graphs exhibit a consistent trend and show a similar level of attenuation, such as a -10 dB response, the slight differences between them may not be significant in terms of practical implications. However, since the primary concern is the -10 dB level, which remains consistent in both cases, it indicates that the system or component is performing as desired within the specified frequency range. In such instances, the small deviations observed between the two graphs may be considered negligible and not have any substantial consequences on the overall functionality or performance of the system. Therefore, the impact of these differences can be deemed insignificant as long as the critical specifications, such as the -10 dB level, are maintained.

Figure 8 depicts the comparison test for S-Parameter S21. Tests on the water phantom section (with and without anomalies) revealed a graph shift caused by irregularities in the water phantom object detected by antenna detection. One of the methods used to simulate abnormalities and facilitate detection testing is the difference in relative permittivity values between the water and air anomaly. The air anomaly has a much lower relative permittivity value than water, making it easier for the antenna to detect and produce a shift in the S-parameter values. This demonstrates the TSA design's effectiveness in detecting anomalies in the water phantom object [4], [18].

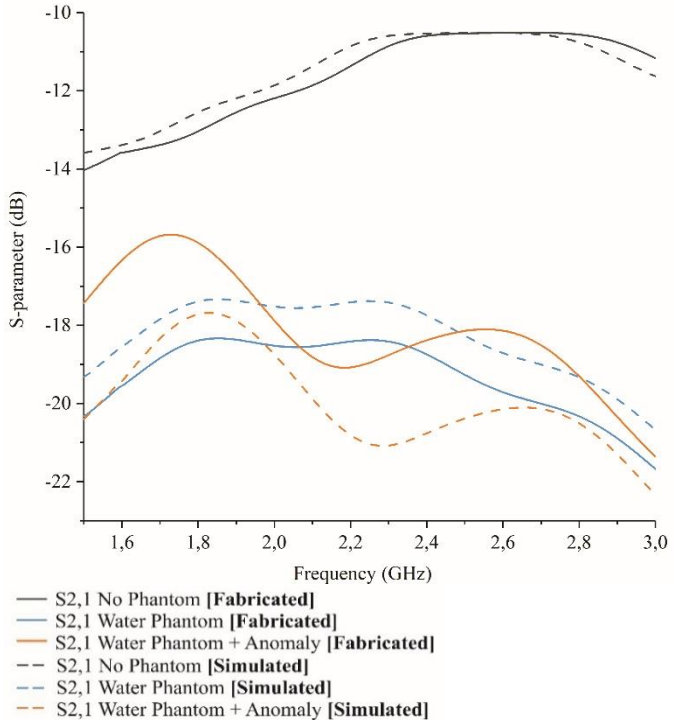

Figure 8. S-Parameter Graph (S2,1) antenna test of various phantoms

When comparing simulation results with real experiments in microwave imaging, it is common to observe slight differences between the two graphs. These disparities arise due to several factors, including the inherent assumptions and simplifications made in the simulation model, as well as the practical limitations and uncertainties encountered during the experimental setup. In simulations, the antenna characteristics, material properties, and environmental factors are typically modelled with certain assumptions and idealized conditions. On the other hand, real-world experiments involve various practical challenges such as imperfections in antenna fabrication, signal losses, measurement errors, and the presence of unwanted noise and interference. These factors can introduce minor discrepancies between the simulated and experimental results. However, despite these differences, the overall trend and essential features of the graphs remain consistent. The key performance parameters and important information, such as the presence of anomalies or variations in the signal response, can still be observed in both the simulation and experimental data. Therefore, while there may be some variations, the end results are fundamentally similar, and the comparison between the simulation and experimental graphs can provide valuable insights into the performance and effectiveness of the microwave imaging system.

With the scattering plot as a graphical representation of the scattered electromagnetic field in a medium, such as biological tissue, when it is irradiated with electromagnetic waves. Tissue anomalies, such as tumours or cysts, can alter the scattering of electromagnetic waves, resulting in a distinct scattering pattern [7].

It is possible to identify these changes in the electromagnetic field and thus detect the presence of anomalies in the tissue by analysing the scattering plot. As a result, scattering plots can give useful information about the internal structure of biological tissues as well as help in illness identification and diagnosis. Anomalies can be discovered using these criteria, much like in earlier investigations [8].

Table IV is the comparison made from previous review study on [5]. Where we compare the dimension, gain and bandwidth and the availability of SAR on the Vivaldi based antennas with FR-4 substrates. For applications utilizing Vivaldi antennas in the 1.7 GHz to 3 GHz frequency range, where cost considerations are paramount, opting for FR-4 as the substrate material can be a practical choice. Despite its limitations, such as reduced performance at very high frequencies, FR-4 offers cost-effectiveness, ease of availability, and compatibility with established manufacturing processes. If the antenna design meets the desired dimensions, gain, and bandwidth requirements while loss considerations can be accommodated, sticking with FR-4 can help maintain a budget-friendly approach without sacrificing overall functionality. However, it is crucial to ensure compliance with regulatory standards, particularly regarding SAR, by consulting relevant guidelines and conducting thorough testing to guarantee safety and performance.

TABLE IV. RESULTS COMPARISON IN THE STUDY

Dimension (mm^2)	Frequency Band (Ghz)	Band width (%)	Gain (dB)	SAR (W/Kg)	Ref
50.8 × 62	1.3–20	175	10	-	[5]
150 × 150	1–4	120	10.74	-	[5]
49 × 48.4	2.9–10.4	112.78	9.58	-	[5]
125 × 100	1.7-3	57	6.09	0.326	This study

To guarantee that the degree of electromagnetic field exposure is within acceptable limits, it is crucial to note that the SAR exposure levels must comply with safety norms and laws. The VTSA's SAR value, which was determined in this work at 0.326 W/kg, is within acceptable bounds and may be employed as a biological detector in an imaging system [4], [18].

Figure 9 provides valuable insights into the quality of antennas for microwave imaging. The anomalies observed in this figure, which represent irregularities in the antenna's S-parameters, hold significant implications. S-parameters are crucial for assessing how an antenna interacts with electromagnetic waves. These anomalies, often seen as spikes, dips, or unexpected patterns, can indicate deviations in the

antenna's performance. Such deviations may include shifts in resonance frequencies, impedance mismatches, or alterations in radiation patterns. These issues can directly affect the antenna's efficiency in transmitting and receiving signals, which, in turn, impacts the quality of microwave imaging [19].

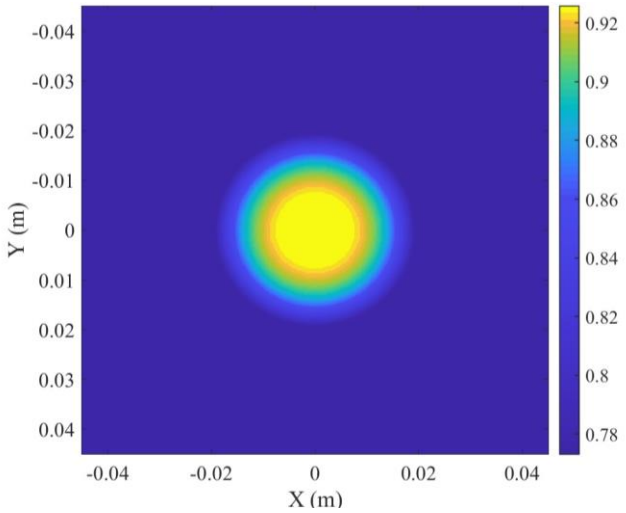

Figure 9. S-Parameter testing with imaging application MERIT

IV. CONCLUSION

This research concluded that tuning the antenna dimensions to optimize the S11 value according to the required performance characteristics may enhance the S11 parameter, VTSA bandwidth, gain and radiation pattern results in the aim of making a well balanced parameters that suggests difference approach. The study also demonstrates that tweaking the S11 value enables you to decrease signal loss while boosting gain, improving the VTSA's overall performance. The ability of the VTSA design to identify anomalies in the water phantom object was demonstrated using the S-parameter test (S21) this result should be better suited. The experiment involved setting up a specific configuration with a defined gap between the antennas and using a suitable VNA within the desired frequency range. The simulation accurately replicated the system's behavior, aligning closely with experimental results. This validation strengthens confidence in the proposed imaging system's effectiveness. Future studies will focus on developing an imaging system tailored to the antenna's specifications.

REFERENCES

[1] W. Ameer, D. Awan, S. Bashir, and A. Waheed, "Use of Directional UWB Antenna for Lung Tumour Detection," *2019 2nd International Conference on Advancements in Computational Sciences (ICACS)*, IEEE, Feb. 2019, pp. 1–5. doi: 10.23919/ICACS.2019.8689137.

[2] A. Janani, A. Darvazehban, S. Rezaeieh, and A. Abbosh, "Focused Planar Electromagnetic Waves for Enhanced Near-Field Microwave Imaging With Verification Using Tapered Gradient-Index Lens Antenna," *IEEE Access*, vol. 10, pp. 86920-86934, 2022, doi: 10.1109/ACCESS.2022.3199002.

[3] B. Basari and S. Ramdani, "Evaluation on Compressive Sensing-based Image Reconstruction Method for Microwave Imaging," *2019 PhotonIcs & Electromagnetics Research Symposium - Spring (PIERS-Spring)*, 2019, pp. 3348–3352, doi: 10.1109/PIERS-Spring46901.2019.9017424.

[4] D. O'Loughlin, M. O'Halloran, B. Moloney, M. Glavin, E. Jones, and A. Elahi, "Microwave Breast Imaging: Clinical Advances and Remaining Challenges," *IEEE Trans Biomed Eng*, vol. 65, no. 11, pp. 2580-2590, 2018, doi: 10.1109/TBME.2018.2809541.

[5] U. Rafique, S. Pisa, R. Cicchetti, O. Testa, and M. Cavagnaro, "Ultra-Wideband Antennas for Biomedical Imaging Applications: A Survey," *Sensors*, vol. 22, no. 9, p. 3230, 2022, doi: 10.3390/s22093230.

[6] M. T. Islam, M. Z. Mahmud, M. T. Islam, S. Kibria, and M. Samsuzzaman, "A Low Cost and Portable Microwave Imaging System for Breast Tumor Detection Using UWB Directional Antenna array," *Sci Rep*, vol. 9, no. 1, p. 15491, 2019, doi: 10.1038/s41598-019-51620-z.

[7] M. Samsuzzaman, M. Islam, M. T. Islam, A. Shovon, M. R. Faruque, and N. Misran, "A 16-modified antipodal Vivaldi antenna array for microwave-based breast tumor imaging applications," *Microw Opt Technol Lett*, vol. 61, no. 9, pp. 2110-2118, 2019, doi: 10.1002/mop.31873.

[8] L. Paul and M. M. Islam, "A Super Wideband Directional Compact Vivaldi Antenna for Lower 5G and Satellite Applications," *Int J Antennas Propag*, vol. 2021, pp. 1-12, 2021, doi: 10.1155/2021/8933103.

[9] F. N. Witriani *et al.*, "Gain Enhancement of Double-Slot Vivaldi Antenna using Corrugated Edges and Semicircle Director for Microwave Imaging Application," *Jurnal Elektronika dan Telekomunikasi*, vol. 21, no. 2, pp. 85-90, 2021, doi: 10.14203/jet.v21.85-90.

[10] J. Abdulameer and A. Alsahlany, "Review: Electromagnetic Radiation Effects on The Human Tissues," *NeuroQuantology*, vol. 20, no. 10, pp. 8130–8146, 2022, doi: 10.14704/nq.2022.20.10.NQ55797.

[11] J. Ren, H. Fan, Q. Tang, Z. Yu, Y. Xiao, and X. Zhou, "An Ultra-Wideband Vivaldi Antenna System for Long-Distance Electromagnetic Detection," *Applied Sciences*, vol. 12, no. 1, p. 528, 2022, doi: 10.3390/app12010528.

[12] S. Kumari and V. Gupta, "Evaluation of Specific Absorption Rate of Microstrip and Monopole Patch Antenna on Human Forearm," *2021 6th International Conference on Communication and Electronics Systems (ICCES)*, Coimbatre, India, 2021, pp. 1666-1670, doi: 10.1109/ICCES51350.2021.9489032.

[13] F. Parveen and P. Wahid, "Design of Miniaturized Antipodal Vivaldi Antennas for Wideband Microwave Imaging of the Head," *Electronics (Basel)*, vol. 11, no. 14, p. 2258, 2022, doi: 10.3390/electronics11142258.

[14] R. Ghatak and A. Gorai, "Binomial stub loaded compact Vivaldi antenna for superwideband applications," *Int J Microw Wirel Technol*, vol. 13, no. 5, pp. 463–468, 2021, doi: 10.1017/S1759078720001257.

[15] A. M. Qashlan, R. W. Aldhaheri, and K. H. Alharbi, "A Modified Compact Flexible Vivaldi Antenna Array Design for Microwave Breast Cancer Detection," *Applied Sciences*, vol. 12, no. 10, p. 4908, 2022, doi: 10.3390/app12104908.

[16] A. Kuriakose, T. A. George and A. S, "Improved High Gain Vivaldi Antenna Design for Through-wall Radar Applications," *2020 International Symposium on Antennas & Propagation (APSYM)*, Cochin, India, 2020, pp. 58-61, doi: 10.1109/APSYM50265.2020.9350711.

[17] J. J. J. Sheela, S. Vanaja, R. Krishnan, V. Avinash., D. Aruna and D. Harini, "Novel Directional Antennas for Microwave Breast Imaging Applications," *2020 International Conference on Smart Electronics and Communication (ICOSEC)*, Trichy, India, 2020, pp. 599-603, doi: 10.1109/ICOSEC49089.2020.9215243.

[18] J. . -C. Chiao et al., "Applications of Microwaves in Medicine," *IEEE Journal of Microwaves*, vol. 3, no. 1, pp. 134-169, 2023, doi: 10.1109/JMW.2022.3223301.

[19] D. O'Loughlin *et al.*, "Open-source software for microwave radar-based image reconstruction," *12th European Conference on Antennas and Propagation (EuCAP 2018)*, 2018, pp. 1–4. doi: 10.1049/cp.2018.0767.